



## Adsorption analysis of PFOA on activated carbon and ion-exchange resin: A comparative study using four isotherm models

KRISTINA B. KASALICA<sup>1#\*</sup>, NATALIJA PETRONIJEVIĆ<sup>2</sup>, JELENA RADULOVIĆ<sup>3</sup>, LATINKA SLAVKOVIĆ BEŠKOSKI<sup>3</sup>, MARIJA B. LJEŠEVIC<sup>1#</sup>, BOJANA MARKOVIĆ<sup>1</sup> and VLADIMIR P. BEŠKOSKI<sup>2#\*\*</sup>

<sup>1</sup>University of Belgrade – Institute of Chemistry, Technology and Metallurgy, National Institute of the Republic of Serbia, Njegoševa 12, Belgrade, Serbia, <sup>2</sup>University of Belgrade – Faculty of Chemistry, Studentski trg 12–16, Belgrade, Serbia and <sup>3</sup>Anahem LTD, Belgrade, Serbia

(Received 20 November, revised 26 November, accepted 1 December 2024)

**Abstract:** Per- and polyfluoroalkyl substances (PFAS), known as “forever chemicals”, are highly persistent environmental pollutants due to their strong carbon–fluorine bonds. Widely used across industries and consumer products, PFAS have accumulated in the environment, raising concerns about their bioaccumulation, toxicity and mobility. Adsorption, particularly using activated carbon and ion exchange resins, is a suitable technique for PFAS removal from contaminated water. This study evaluates the sorption efficiency of granular and powdered activated carbon and two ion exchange resins to identify the most effective materials for remediation. All tested sorbents showed great performance, however Amberlite IRA 402, and powdered activated carbon K/B were the most efficient. Based on the isotherm models used, it is suggested that physisorption is a dominant process, where the multilayer adsorption on a heterogeneous surface is being favoured.

**Keywords:** immobilization; PFAS; water remediation.

### INTRODUCTION

Per- and polyfluoroalkyl substances (PFAS), often known as “forever chemicals”, are a group of manmade compounds currently under intense scrutiny. PFAS comprise thousands of individual chemicals, valued for their unique commercial properties, such as heat resistance and water- and grease-repellent qualities.<sup>1</sup> In the last several decades, PFAS are widely used across industries, inc-

\* Corresponding authors. E-mail: (\*)kristina.kasalica@ihtm.bg.ac.rs;  
(\*\*)vbeskoski@chem.bg.ac.rs

# Serbian Chemical Society member.  
<https://doi.org/10.2298/JSC241120097K>

luding construction, electronics, oil and gas, mining, semiconductors, recycling and transportation. They are also integral to producing ceramics, nanostructures, explosives, firefighting foams, medical devices, plastics, rubbers and refrigerants. In daily life, PFAS are present in adhesives, cleaning products, coatings, paints, cosmetics, personal care items, food packaging, pesticides, fertilizers and textiles. Their extensive use underscores their essential role in modern society, necessitating closer investigation of their production and environmental impact.<sup>2</sup> However, despite the highly valuable and important properties that have led to the widespread use of these compounds, one characteristic stands out in particular – their persistence in the environment. Namely, due to the strength of their carbon-fluorine bonds, all PFAS exhibit environmental persistence, with many being bioaccumulative, highly mobile and toxic. Their widespread use has led to their presence across various environmental compartments, complicating efforts to manage them.<sup>3</sup> Significant efforts are being made to regulate the use of PFAS compounds in industry,<sup>4</sup> but at the same time it is essential to focus on the environment where these compounds have already accumulated.

One of the most studied methods for PFAS removal from water is adsorption. Adsorption involves the physical or chemical interaction between a solid surface (adsorbent) and a solute (adsorbate), where the adsorbate in this context is a pollutant in an aqueous solution. This technique enables the efficient treatment of large volumes of water in a straightforward and compact manner, with manageable costs.<sup>5</sup> Adsorption of PFAS could be performed using carbon-based materials (activated carbon, carbon nanotubes), ionic surfactants, anion exchange resins, composite materials but the overall efficacy depends on PFAS that are present in the environment, matrix characteristics as well as the properties of material used.<sup>6,7</sup> Sorbents bind PFAS mainly through hydrophobic and electrostatic interactions, and their effectiveness often depends on surface area and porosity.<sup>8,9</sup> In addition to adsorption, ion exchange process using ion exchange resins (IER) has received a lot of attention in the past couple of years.<sup>8</sup> The immobilization of PFAS onto a sorbent has proven to be very efficient and easy to apply, however this method does not destroy PFAS, opening the question of safe disposal or possible reuse of the sorbent after the sorption process. However, given the very low concentrations of PFAS in the environment, the immobilization could serve as an effective preliminary step for other remediation technologies that are unsuitable for addressing low-level contamination in terms of their associated remediation costs.<sup>10</sup> Hence the aim of this study was to evaluate the sorption efficiency of granular and powdered activated carbon, along with two ion exchange resins, to identify the most effective sorbent for future research on treating contaminated materials. Additionally, sorption behaviour of the sorbents that were most efficient in adsorbing of PFOA used as PFAS model compound was investigated. Removing PFAS from water not only reduces their mobility

and bioavailability but also promotes the desorption of PFAS from sediments, facilitating sediment purification and contributing to a comprehensive remediation strategy for contaminated environments.

## EXPERIMENTAL

### Chemicals

Perfluorooctanoic acid (PFOA) was purchased from Sigma–Aldrich, Cat. No. 171468. Two types of activated carbon obtained from Trayal Corporation, Serbia, were used, granular activated carbon (KRF), as activated carbon in grain with particle size 0.25–1.0 mm, produced from carbonized coconut shell, activated by the water steam in static furnace, and powdered activated carbon (K/B powder), screen size of 0.080 mm at max. 70 %, produced from the same material and activated by the water steam in static furnace. Ion exchange resins: Amberlite® IRA402 chloride form, product number: 06466, batch number: bccg5078, brand: SIAL, CAS number: 52439-77-7, particle size: 600–750 µm, was purchased from Supelco and Amberlite® IRA67 free base – gel form, 16–50 mesh (wet), product number: A9960, batch number: SLCB3374, brand: SIGMA, CAS number: 65899-87-8, MDL number: MFCD00145567, was purchased from Sigma–Aldrich. Native perfluorooctanoic acid standard and labelled standard of perfluoro-*n*-(<sup>13</sup>C8) octanoic acid, M8PFOA were purchased from Wellington Laboratories Inc.

### Study design

A batch test to assess the adsorption of PFOA was performed by weighing 50 mg each of Amberlite IRA 402, Amberlite IRA 67 ionic exchange resin (activated overnight in distilled water) KRF and K/B powder into 50 mL vials and 25 mL of 100 mg/L PFOA. The experiment was conducted at the rotary shaker with 200 rpm during 24 h, after which an aliquot of 5 mL was filtered through 0.22 µm PP syringe filter and stored at 4 °C until analysis where the remaining concentration of PFOA was determined.

Additional batch tests were set up similarly to determine the behaviour of most efficient sorbents on different temperatures and with varying concentration of PFOA (5–35 ppm). The experiment was conducted at two temperatures, 4 and 28 °C, at the rotary shaker with 200 rpm during 24 h, after which an aliquot of 5 mL was filtered through 0.22 µm PP syringe filter and stored at 4 °C until analysis.

### Isotherm models

The collected equilibrium data were analyzed using Langmuir, Freundlich, Temkin and Dubinin–Radushkevich isotherm models to identify the mechanisms that control the PFOA adsorption process.<sup>11</sup> The Langmuir adsorption isotherm model treats the adsorption process as a chemical phenomenon, assuming that adsorption occurs on a homogeneous surface of the adsorbent and is limited to the formation of a monolayer. On the other hand, the Freundlich isotherm model describes multilayer adsorption on a heterogeneous adsorbent surface. The Temkin isotherm assumes that the heat of adsorption for all molecules on the adsorbent surface decreases linearly with coverage due to adsorbate–adsorbent interactions. This model is characterized by multilayer adsorption with a uniform distribution of binding energies. The Dubinin–Radushkevich model can describe adsorption on heterogeneous surfaces and provides valuable insights into the energy distribution and nature of the adsorption process. The OriginPro 2021 Software was used for the isotherms' linear regression analyses. Two error functions, the coefficient of determination ( $R^2$ ) and chi-square ( $\chi^2$ ) test, were used to ensure

accurate and consistent estimations for fitting the experimental data to the investigated isothermal models.<sup>12</sup>

*Liquid chromatography coupled to tandem mass spectrometry*

Quantitative analysis of PFOA was performed using a Thermo Scientific Accela high performance liquid chromatograph (HPLC) with a triple quadrupole mass analyser TSQ Quantum Access MAX (Thermo Fisher Scientific, USA). The column used was a Waters Acquity UPLC BEH Shield RP18 Column, (130 Å, 1.7 µm, 2.1 mm×100 mm, Waters, USA) equipped with security guard ultra holder for UHPLC Columns (2.1 to 4.6 mm, Phenomenex, USA) with SecurityGuard ULTRA cartridges for EVO-C18 and elution was performed using a mobile phase consisting of ultrapure water, 0.1 % HCOOH, 5 mM HCOONH<sub>4</sub> (solution A) and MeOH, 0.1 % HCOOH, 5 mM HCOONH<sub>4</sub> (solution B) as follows: 0 min: 72 % A, 28 % B; 4.5 min: 15 % A, 85 % B; 4.6 min: 1 % A, 99 % B; 10 min: 1 % A, 99 % B; 12 min: 72 % A, 28 % B. The column flow was 250 µL/min and column temperature 40 °C. The ionization was performed in H-ESI mode. The mass spectrometer operated in negative ionization mode. M8PFOA was used as an injection standard. Parameters of MS/MS analysis are given in the Table I. Prior to injection, the samples were filtered through 0.22 µm PP syringe filters, previously rinsed with methanol. Data analyses were performed using Thermo Xcalibur 3.0.63, 2014 software (Thermo Fisher Scientific, USA).

TABLE I. MS/MS parameters for PFOA analysis

Parameter	PFOA	M8PFOA
Standard type	Native standard	Injection standard
Retention time, min	4.21	4.21
Parent ion ( <i>m/z</i> )	413	421
Quantification ion ( <i>m/z</i> )	369	376
Confirmation ion ( <i>m/z</i> )	169	172
Cone voltage, eV	10	10
Collision energy Q1, eV	17	18
Collision energy Q2, eV	10	10
Scan time, s	0.05	0.05
Scan width ( <i>m/z</i> )	0.2	0.2

## RESULTS AND DISCUSSION

Batch test for assessing the adsorption efficacy of four different sorbents was investigated, and the results are shown in the Table II. The PFOA concentrations remaining after the incubation period adsorption onto activated carbons are extremely low, with the adsorption efficiency reaching over 95 % for all tested activated carbons. Ion exchange resins were also very effective in the PFOA adsorption, with over 90 % adsorption with IRA 67 and 99 % with IRA 402.

Since the best adsorption results were obtained using IRA 402 and K/B powder, these two sorbents were investigated in more detail. Four commonly used isotherm models, Langmuir, Freundlich, Temkin and Dubinin–Radushkevich, were applied to analyse and discuss experimentally obtained data. The values of the calculated isotherm parameters and the corresponding error functions for PFOA on K/B and IRA 402 are given in Tables III and IV, respectively.

TABLE II. Results of the batch adsorption test using different sorbents

Sorbent	PFOA concentration, mg/L	Adsorption of PFOA, %
KRF	4.65	95.35
K/B powder	1.05	98.95
IRA 67	9.02	90.98
IRA 402	0.34	99.66

TABLE III. Parameters of the Langmuir, Freundlich, Temkin and Dubinin–Radushkevich isotherm models of PFOA adsorption on K/B

Isotherm	Parameter	Value	
Langmuir	$t / ^\circ\text{C}$	28	4
	$q_{\text{m,L}} / \text{mg g}^{-1}$	12.75	11.74
	$K_{\text{L}} / \text{L mg}^{-1}$	5.98	16.71
	$R_{\text{L}}$	$1.10 \times 10^{-2}$	$3.99 \times 10^{-3}$
	$R^2$	0.827	0.685
	$\chi^2$	1.107	2.150
Freundlich	$q_{\text{m,L}} / \text{mg g}^{-1}$	12.75	11.74
	$K_{\text{F}} / \text{dm}^3 \text{g}^{-1}$	9.34	10.46
	$n$	2.95	3.51
	$R^2$	0.949	0.922
	$\chi^2$	0.527	0.703
	$K_{\text{T}} / \text{dm}^3 \text{g}^{-1}$	56,61	162.10
Temkin	$b_{\text{T}} / \text{kJ mol}^{-1}$	0.96	1.03
	$R^2$	0.969	0.937
	$\chi^2$	0.268	0.540
Dubinin–Radushkevich	$q_{\text{m,DR}} / \text{mg g}^{-1}$	12.43	12.37
	$K_{\text{DR}} / \text{mol}^2 \text{J}^{-2}$	$2.58 \times 10^{-8}$	$1.81 \times 10^{-8}$
	$E / \text{kJ mol}^{-1}$	4.40	5.26
	$R^2$	0.811	0.775
	$\chi^2$	1.312	1.585
	C3a	D3	30

As can be seen from Fig. 1, the Langmuir adsorption isotherms for K/B and IRA 402 showed good agreement with experimental data at low initial concentration values (5–20 ppm). At higher initial concentrations of PFOA, the experimental data show a deviation from the Langmuir model, which indicates that the adsorption process continues even after the formation of a monolayer on the active sites. The Langmuir constant ( $K_{\text{L}}$ ) is a measure of the adsorption energy. Lower  $K_{\text{L}}$  values for IRA 402 adsorbent (0.02 L/mg for 28 °C and  $3.73 \times 10^{-3}$  L/mg for 4 °C) indicate that physisorption is more dominant than chemisorption during PFOA adsorption. The value of the dimensionless separation factor ( $R_{\text{L}}$ ), indicates the adsorption nature as favourable ( $0 < R_{\text{L}} < 1$ ), linear ( $R_{\text{L}} = 1$ ) or irreversible ( $R_{\text{L}} = 0$ ).  $R_{\text{L}}$  values for K/B and IRA 402 range from  $3.99 \times 10^{-3}$  to 0.93 indicating that adsorption is favoured.

TABLE IV. Parameters of the Langmuir, Freundlich, Temkin and Dubinin-Radushkevich isotherm models of PFOA adsorption on IRA 402

Isotherm	Parameter	Value	
Langmuir	$t / ^\circ\text{C}$	28	4
	$q_{m,L} / \text{mg g}^{-1}$	51.28	123.45
	$K_L / \text{L mg}^{-1}$	0.02	$3.73 \times 10^{-3}$
	$R_L$	0.71	0.93
	$R^2$	0.859	0.767
	$\chi^2$	1.509	1.389
Freundlich	$q_{m,L} / \text{mg g}^{-1}$	51.28	123.45
	$K_F / \text{dm}^3 \text{g}^{-1}$	1.41	0.61
	$n$	1.30	1.17
	$R^2$	0.862	0.775
	$\chi^2$	1.236	1.252
	$K_T / \text{dm}^3 \text{g}^{-1}$	0.81	0.48
Temkin	$b_T / \text{kJ mol}^{-1}$	0.62	0.73
	$R^2$	0.871	0.808
	$\chi^2$	0.828	0.760
	$q_{m,DR} / \text{mg g}^{-1}$	9.39	6.58
	$K_{DR} / \text{mol}^2 \text{J}^{-2}$	$1.77 \times 10^{-6}$	$4.34 \times 10^{-6}$
	$E / \text{kJ mol}^{-1}$	0.53	0.34
Dubinin–Radushkevich	$R^2$	0.818	0.743
	$\chi^2$	0.935	0.962
	C3a	9.39	6.58

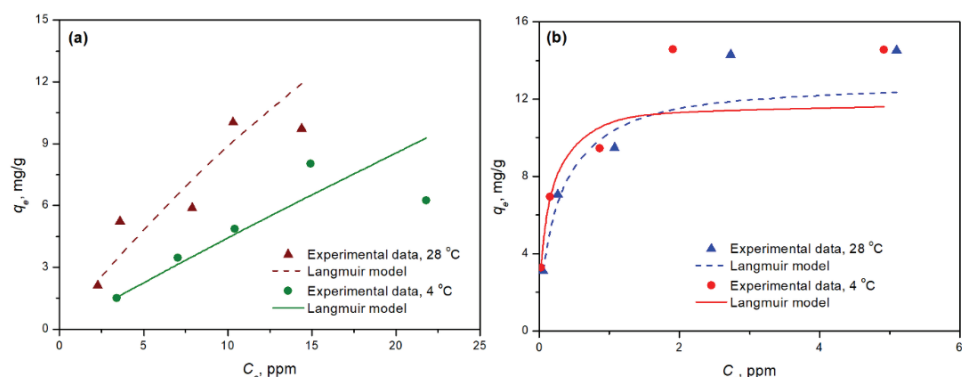


Fig. 1. Langmuir adsorption isotherms for: a) IRA 402 and b) K/B at 28 and 4 °C (conditions:  $C_o$ , 5–35 ppm,  $m_{\text{ads}} = 50 \text{ mg}$ ,  $V = 25 \text{ ml}$ ,  $\tau = 24 \text{ h}$ ).

The low values of the coefficient of determination and high values of the chi-square test for the Langmuir isotherm model mean that the applied isotherm could not be used to predict the PFOA adsorption process on both adsorbents. Therefore, linear fitting of the Freundlich adsorption isotherm model was applied to the experimental data. The results are shown in Fig. 2.

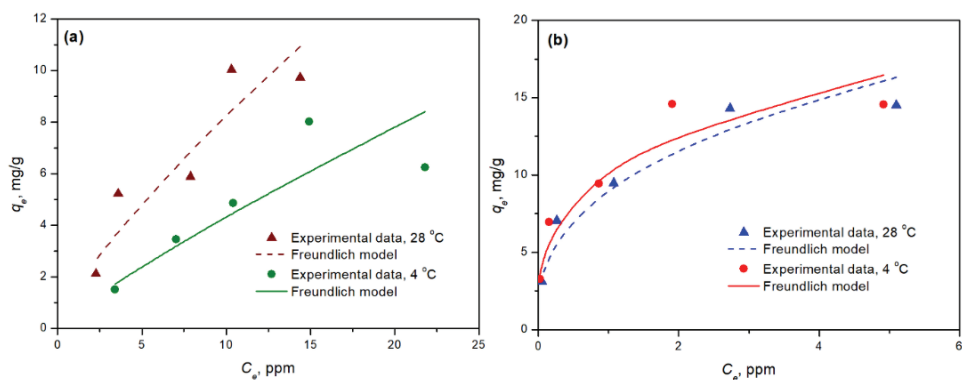


Fig. 2. Freundlich adsorption isotherms for: a) IRA 402 and b) K/B at 28 and 4 °C (conditions:  $C_o$ , 5–35 ppm,  $m_{ads}$  = 50 mg,  $V$  = 25 ml,  $\tau$  = 24 h).

Based on the  $R^2$  and  $\chi^2$  values for the Freundlich adsorption isotherm, the adsorption isotherms show a slightly better agreement with the experimental results compared to the Langmuir model on both materials and at both tested temperatures, which indicates that the adsorption takes place on a heterogeneous surface through multilayer adsorption. The Freundlich constant ( $K_F$ ) indicates the adsorption strength. Based on the obtained results for  $K_F$  values, it can be concluded that a higher adsorption capacity is achieved with K/B adsorbent than with IRA 402, which is in accordance with the experimentally obtained data. Likewise, based on the  $1/n$  value, which is in the range of 0.28 to 0.85, it can be concluded that the analysed adsorption processes on K/B and IRA 402 adsorbent are favoured.<sup>11</sup> The heterogeneous nature of adsorption increases with decreasing temperature because the value of  $1/n$  is lower at lower temperatures, as can be seen from Tables III and IV.

Further, the experimental data were also analysed by the Temkin adsorption isotherm model. Graphic representations of experimental results fitted with a linearized form of the Temkin isotherm model for PFOA adsorption on K/B and IRA 402 are shown in Fig. 3. Based on the obtained results shown in Tables III and IV for  $R^2$  and  $\chi^2$ , it can be concluded that the mentioned model best describes the adsorption processes at both investigated temperatures for K/B and IRA 402 adsorbents. The  $b_T$  values are greater than 0, which indicates exothermic adsorption processes. The higher  $K_T$  values for the K/B adsorbent at both investigated temperatures suggest a greater adsorption capacity for PFOA compared to that of IRA 402.

The Dubinin–Radushkevich adsorption isotherm model was used to determine the type of adsorbate–adsorbent interaction during the adsorption process. Fig. 4 shows the fitting curves of linear regression for PFOA adsorption onto IRA 402 and K/B adsorbents. The values of the Dubinin–Radushkevich constant

( $K_{DR}$ ) for K/B adsorbent were  $2.58 \times 10^{-8}$  and  $1.81 \times 10^{-8}$  mol<sup>2</sup>/J<sup>2</sup>, while for IRA 402 amounted to  $1.77 \times 10^{-6}$  and  $4.34 \times 10^{-6}$  mol<sup>2</sup>/J<sup>2</sup> at 28 and 4 °C, respectively. Based on the obtained  $K_{DR}$  values, the energies of the adsorption processes ( $E$ ) were determined. The values of  $E$  for the PFOA adsorption on K/B and IRA 402 adsorbents range from 0.34 to 5.26 kJ/mol, which corresponds to physisorption ( $E < 8$  kJ/mol).<sup>13</sup>

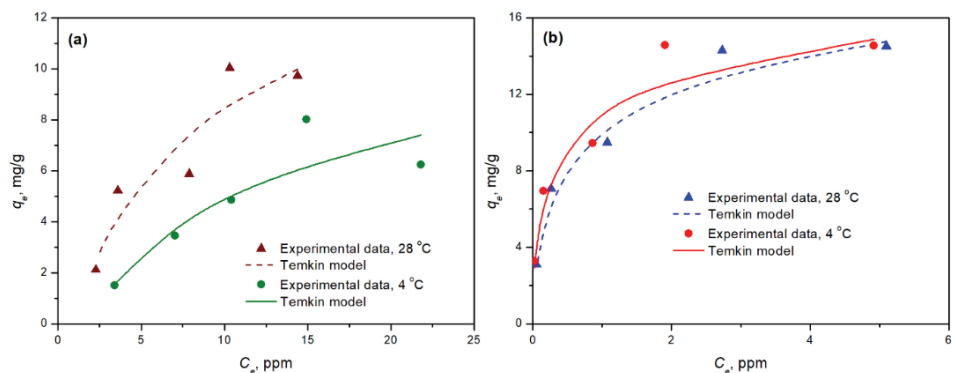


Fig. 3. Temkin adsorption isotherms for: a) IRA 402 and b) K/B at 28 and 4 °C (conditions:  $C_o$ , 5–35 ppm,  $m_{ads}$  = 50 mg,  $V$  = 25 ml,  $\tau$  = 24 h).

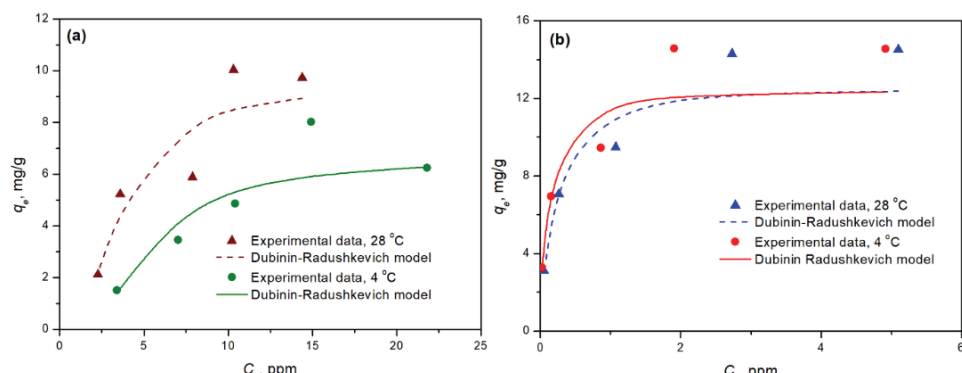


Fig. 4. Dubinin–Radushkevich adsorption isotherms for: a) IRA 402 and b) K/B at 28 and 4 °C (conditions:  $C_o$ , 5–35 ppm,  $m_{ads}$  = 50 mg,  $V$  = 25 ml,  $\tau$  = 24 h).

## CONCLUSION

This study applied four well-known two-parameter isotherm models to better understand the PFOA adsorption mechanism onto K/B and IRA 402 adsorbents. The Langmuir isotherm model showed compatibility with experimental data at low PFOA concentrations, supporting monolayer adsorption on a homogeneous surface. However, deviations at higher concentrations, indicated by low  $R^2$  values and high chi-square values, suggest multilayer adsorption or interactions

beyond a single monolayer. The Freundlich model provided a slightly better fit, suggesting multilayer adsorption on a heterogeneous surface, as supported by the Freundlich constant ( $K_F$ ) and  $1/n$  values (0.28–0.85), which indicate favourable adsorption, especially at lower temperatures. This temperature dependence further highlights the heterogeneous nature of the adsorption sites. The Temkin model best described the adsorption processes for both adsorbents at all temperatures, indicating exothermic and multilayer adsorption, as reflected in the positive  $b_T$  values. The higher  $K_T$  values for the K/B adsorbent indicate a greater adsorption capacity for PFOA compared to that of IRA 402. Lastly, the Dubinin–Radushkevich model helped confirm that the adsorption process primarily involves physisorption, as the energy values ( $E$ ) were consistently below 8 kJ/mol. In conclusion, PFOA adsorption on K/B and IRA 402 follows a predominantly physisorption process, with multilayer adsorption on a heterogeneous surface being favoured, particularly for K/B. This understanding of adsorption mechanisms and affinities across isotherm models can form more effective adsorbent selection and optimization for PFOA removal in future applications.

*Acknowledgements.* This research was supported by Project “VISION” funded by the company Solvay Specialty Polymers Italy S.p.A. The activated carbons were obtained from the Trayal Corporation, Serbia.

#### ИЗВОД

#### АНАЛИЗА АДСОРПЦИЈЕ РФОА НА АКТИВНОМ УГЉЕНИКУ И ЈОНОИЗМЕЊИВАЧКИМ СМОЛАМА: УПОРЕДНА СТУДИЈА НА ОСНОВУ ЧЕТИРИ МОДЕЛА ИЗОТЕРМИ

КРИСТИНА Б. КАСАЛИЦА<sup>1</sup>, НАТАЛИЈА ПЕТРОНИЈЕВИЋ<sup>2</sup>, ЈЕЛЕНА РАДУЛОВИЋ<sup>3</sup>, ЛАТИНКА СЛАВКОВИЋ  
БЕШКОСКИ<sup>3</sup>, МАРИЈА Б. ЉЕШЕВИЋ<sup>1</sup>, БОЈАНА МАРКОВИЋ<sup>1</sup> и ВЛАДИМИР П. БЕШКОСКИ<sup>2</sup>

<sup>1</sup>Универзитет у Београду – Институт за хемију, технолоџију и металургију, Институт ог  
националној значају за Републику Србију, Нвејшева 12, Београд, <sup>2</sup>Универзитет у Београду –  
Хемијски факултет, Студентски трг 12–16, Београд и <sup>3</sup>Анахем доо, Београд

Пер- и полифлуороалкилна једињења (PFAS), позната као „вечне хемикалије“, представљају дуготрајне загађујуће супстанце услед присуства јаких угљеник–флупор веза. Ова једињења су нашла широку употребу у индустрији и роби широке потрошње те су тако ослобођена и у животну средину, што је довело до забринутости због њихове биоакумулације, токсичности и мобилности. Адсорпција, посебно коришћењем активног угља и јонизмењивачких смола, представља погодну технику за уклањање PFAS из контаминиране воде. У овој студији проценета је ефикасност сорпције гранулисаног и прашкастог активног угља, као и две јонизмењивачке смоле, како би се идентификовали најефикаснији материјали за ремедијацију. Сви тестиирани сорбенти показали су одличне резултате, али су Ambelite IRA 402 и прашкасти активни угљ K/B били најефикаснији. На основу примењених изотермских модела, закључак је да је физисорпција доминантан процес, при чему је фаворизована мултислојна адсорпција на хетерогеној површини.

(Примљено 20. новембра, ревидирано 26. новембра, прихваћено 1. децембра 2024)

## REFERENCES

1. Z. Wang, A. M. Buser, I. T. Cousins, S. Demattio, W. Drost, O. Johansson, K. Ohno, G. Patlewicz, A. M. Richard G. W. Walker, G. S. White, E. Leinala, *Environ. Sci. Technol.* **55** (2021) 15575 (<https://doi.org/10.1021/acs.est.1c06896>)
2. L. G. T. Gaines, *Am. J. Ind. Med.* **66** (2023) 353 (<https://doi.org/10.1002/ajim.23362>)
3. I. J. Neuwald, D. Hübner, H. L. Wiegand, V. Valkov, U. Borchers, K. Nödler, M. Scheurer, S. E. Hale, H. P. H. Arp, D. Zahn, *Environ. Sci. Technol.* **56** (2022) 6380 (<https://doi.org/10.1021/acs.est.1c07949>)
4. ECHA, <https://echa.europa.eu/hot-topics/perfluoroalkyl-chemicals-pfas> (accessed 15.11.2024)
5. I. Ali, M. Asim, T.A. Khan, *J. Environ. Manage.* **113** (2012) 170 (<https://doi.org/10.1016/j.jenvman.2012.08.028>)
6. N. Bolan, B. Sarkar, Y. Yan, Q. Li, H. Wijesekara, K. Kannan, D.C.W. Tsang, M. Schauerte, J. Bosch, H. Noll, Y. S. Ok, K. Scheckel, J. Kumpiene, K. Gobindlal, M. Kah, J. Sperry, M. B. Kirkham, H. Wang, Y. F. Tsang, D. Hou, J. Rinklebe, *J. Hazard. Mater.* **401** (2021) 123892 (<https://doi.org/10.1016/j.jhazmat.2020.123892>)
7. R. Mahinroosta, L. Senevirathna, *J. Environ. Manage.* **255** (2020) 109896 (<https://doi.org/10.1016/j.jenvman.2019.109896>)
8. F. Dixit, R. Dutta, B. Barbeau, P. Berube, M. Mohseni, *Chemosphere* **272** (2021) 129777 (<https://doi.org/10.1016/j.chemosphere.2021.129777>)
9. E. Barth, J. McKernan, D. Bless, K. Dasu, *J. Environ. Manage.* **296** (2021) 113069 (<https://doi.org/10.1016/j.jenvman.2021.113069>)
10. V. Beškoski, M. Lješević, B. Jiménez, J. Muñoz-Arnanz, P. Colomer-Vidal, H. Inui, T. Nakano, in *Soil Remediation Science and Technology. The Handbook of Environmental Chemistry*, Vol 130, J. J. Ortega-Calvo, F. Coulon, Eds., Springer Nature, Cham, 2024, p.332 ([https://doi.org/10.1007/698\\_2023\\_1070](https://doi.org/10.1007/698_2023_1070))
11. E. E. Jasper, V. O. Ajibola, J.C. Onwuka, *Appl. Water. Sci.* **10** (2020) 132 (<https://doi.org/10.1007/s13201-020-01218-y>)
12. A. Nastasović, B. Marković, Lj. Suručić, A. Onjia, *Metals* **12** (2022) 814 (<https://doi.org/10.3390/met12050814>)
13. M. Shafiq, A. A. Alazba, M. T. Amin, *Sustainability* **13** (2021) 3785 (<https://doi.org/10.3390/su13073785>).